Appendix A

We here consider how the position dependency of the detected tracks affects the density results.

The fill factor (i.e., track detection efficiency in a film) of the base tracks also depends on the position of the scanned film. The typical causes of the inefficiency are heterogeneous thickness of the emulsion layers, some dusts or scratches on the emulsion surface, and the poorly tuned parameters for the scanning.

Fig. 15 shows the position distribution of the fill factor of all films of an ECC. For example, at upper right the films tend to have the low fill factor (e.g., a-f, h, k, l, q). This part has the larger thickness of emulsion layer because drips were left in the upper right corner when drying after soaking with glycerin solution. Fig. 15(s) and (t) have larger area of low fill factor in the right and left. The reason might be the poorly tuned parameters for the scanning.

Compared to the size of the scoria cone, the ECC is a very small "element", thus the local position dependence of the fill factor can be approximately treated as an average fill factor $\varepsilon_j(\theta_x, \theta_y)$. The inefficiency of the basetrack is reflected in the $\varepsilon_j(\theta_x, \theta_y)$ in Eq. (4). Finally, $\varepsilon_j(\theta_x, \theta_y)$, which encompasses the effects of the local inefficiency of the basetrack, is effectively used to derive the angle-dependent muon detection efficiency.

How about the position dependency of noise? Local high density of random silver grains caused by any chemical conditions, or fake images produced by scratches on the films might create a group of fake tracks concentrated in one place. Such fake tracks tend to have small slopes by scanning with automated emulsion readout system. If such noise is continuous at the same location on the film, they will make many parallel tracks at a certain slope and give a systematic error in the result. However, such possibility has been eliminated by the track selection algorithm described in the section 4.2. Because such concentrated tracks in position and angular space make numerous entangled linklets. Branches in track connections were removed in the selection. Fig. 16 shows the number of selected tracks with small slope per mm^2 in each observation site. There are no remarkable spikes. The difference of the peak in the histograms depends on the difference of exposure time (SE, W, NNE), existence of topography in the backward direction (NE), and pitch angle of the detector attitude (i.e., SW has large pitch angle, thus less tracks of the small slopes).

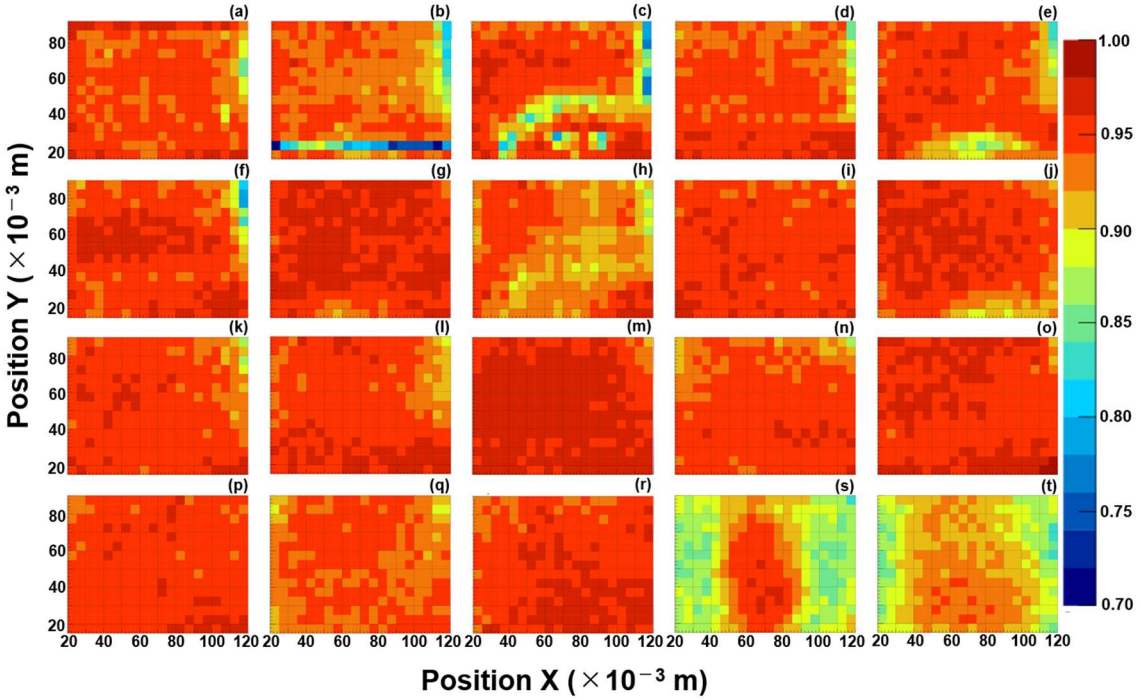

Figure 15. The position distribution of the fill factor in each film of ECC02. (a)–(t) represent PL01–PL20, respectively.

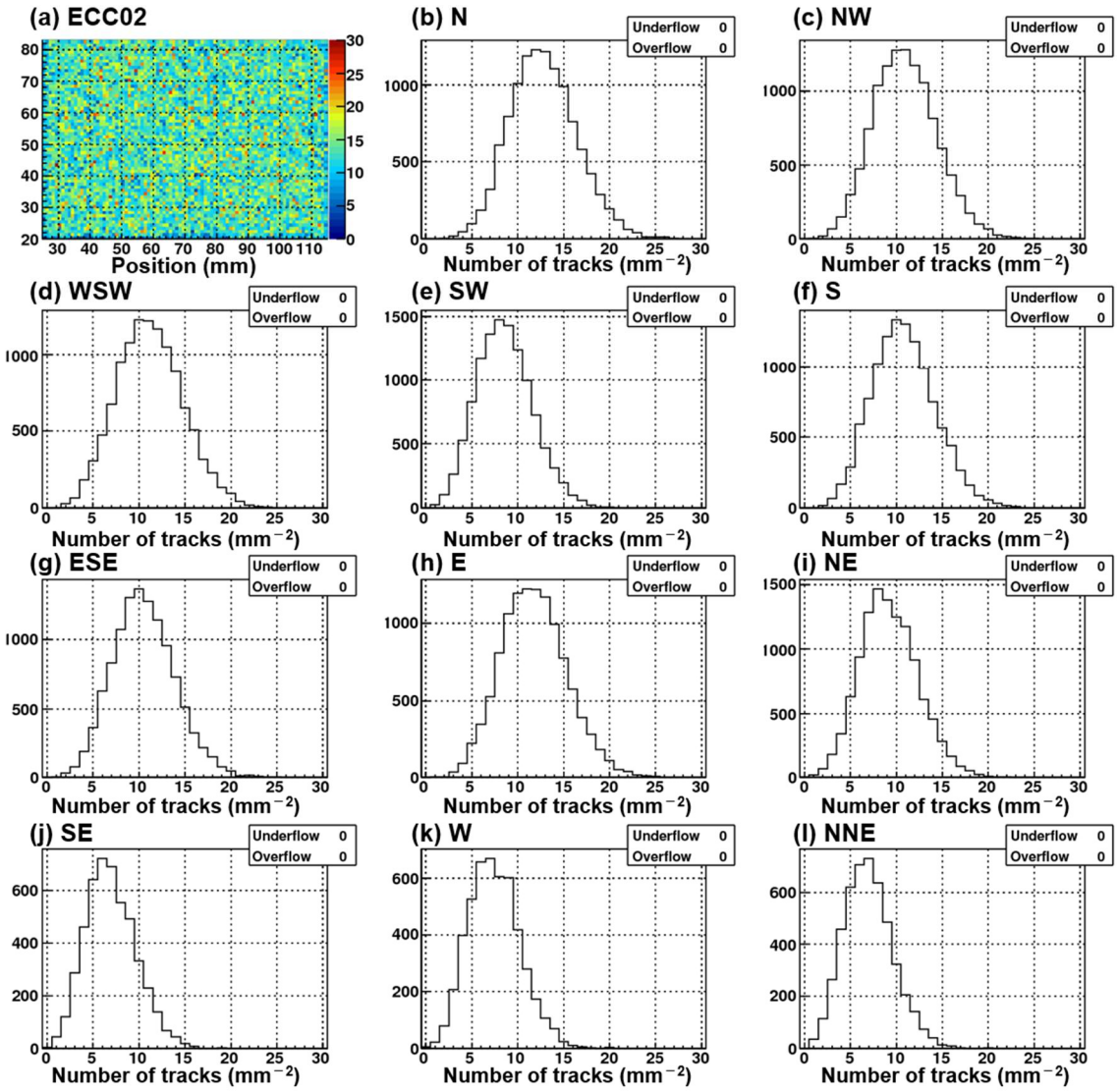

Figure 16. (a) The position distribution of the number of the selected tracks per mm^2 in the ECC02. (b)–(l) The number of the selected tracks per mm^2 of the site N–NNE, respectively. These tracks selected for this figure come from in the backward direction, and have small slopes, $|\tan\theta_x| < 0.5$, and $|\tan\theta_y| < 0.5$.